Available online at www.sciencedirect.com
ScienceDirect
Biochimica et Biophysica Acta 1778 (2008) 405–413
Biochimica et Biophysica Acta
BBA
www.elsevier.com/locate/bbamem

Electrogenic steps of the SR Ca-ATPase enzymatic cycle and the effect of curcumin

Gianluca Bartolommei, Francesco Tadini-Buoninsegni, Maria Rosa Moncelli, Rolando Guidelli *

Department of Chemistry, University of Florence, via della Lastruccia 3, 50019 Sesto Fiorentino (FI), Italy

Received 30 January 2007; received in revised form 10 October 2007; accepted 17 October 2007
Available online 25 October 2007

Abstract

Sarcoplasmic reticulum (SR) vesicles were adsorbed on an octadecanethiol/phosphatidylcholine mixed bilayer anchored to a gold electrode, and the Ca-ATPase contained in the vesicles was activated by ATP concentration jumps in the presence of calcium ions. The resulting capacitive current transients are compared with those calculated on the basis of the enzymatic cycle of the calcium pump. This comparison provides information on the kinetics of the E_2–E_1 conformational change and on its pH dependence. The alteration in the current transients following ATP concentration jumps in the presence of curcumin is examined. In particular, curcumin decreases the rate of slippage of the Ca-ATPase, and at concentrations above 10 μM reduces calcium transport by this pump.

Keywords: SERCA; Electrogenic transport; Curcumin; Solid supported membrane

1. Introduction

The Ca-ATPase of the sarcoplasmic reticulum (SR) is a membrane protein that couples the hydrolysis of a molecule of ATP to the active transport of two Ca^{2+} ions from the cytoplasm to the lumen of the SR, thereby promoting muscle relaxation [1–3]. The enzymatic cycle of this calcium pump has been extensively investigated, mainly by biochemical methods. Thus, the phosphoenzyme intermediate has been determined by incorporation of [γ-^{32}P]ATP terminal phosphate onto Ca-ATPase, or by its backdoor phosphorylation with [^{32}P]P_i in the absence of calcium [4–7]. Calcium binding to the pump and its translocation have been determined using Ca^{2+} isotopes [8–11] or fluorescent probes [11–13]. The E_1/E_2 equilibrium and kinetics have been measured using Ca-ATPase labeled with fluorescent probes or exploiting tryptophan fluorescence [14,15]. All these biochemical methods have allowed a detailed picture of the different steps of the enzymatic cycle to be obtained [16–21]. The equilibrium and rate constants of many of these steps have been adjusted so as to match the experimental data obtained by the above methods. A limitation of biochemical methods is represented by their being insensitive to electrogenic steps.

Ca-ATPase electrogenicity was investigated by Apell and coworkers by carrying out equilibrium and kinetic measurements on vesicles incorporating Ca-ATPase in the presence of styryl dyes [22–26]; the fluorescence of these dyes varies with a change in the local electric field within the protein/membrane dielectric, and hence with a change in the charge of the protein. A more direct, electrophysiological procedure to measure the electrogenicity of ion pumps and transporters was devised by Pintschovius and Fendler [27,28] and has been extensively adopted by Fendler and coworkers [29–32] and by the present authors [33–36]. It consists in carrying out concentration jumps of activating substances on proteoliposomes adsorbed on a mixed alkanethiol/phospholipid bilayer supported by a gold electrode (the solid supported membrane, SSM). The concentration jump induces the flow of a capacitive current that is recorded against time. The resulting current transient exhibits a relatively steep rising section, followed by a current peak and by a descending branch. Integration of the current transient measures the charge moved by the activating substance.

A concentration jump consists in the rapid flow of a solution of an activating substance, which reaches the electrode surface

* Corresponding author. Tel.: +39 055 4573097; fax: +39 055 4573385.
E-mail address: guidelli@unifi.it (R. Guidelli).

0005-2736/$ - see front matter © 2007 Elsevier B.V. All rights reserved.
doi:10.1016/j.bbamem.2007.10.016

through a narrow tube upon expelling a "non-activating" solution differing from the activating one only by the absence of the activating substance. The temporary contact of the boundary region between the two solutions with the electrode surface causes the concentration of the activating substance to increase rapidly from a practically zero value to its limiting, bulk value. This non-instantaneous concentration jump is unavoidable, and so far it has been regarded as the only cause of the rising section of the current transients. Consequently, the concentration of the activating substance at the current peak has been corrected on the basis of this assumption. As a matter of fact, the activation of the pump may well start from an electrosilent step: in this case, the current will not increase instantaneously even in the presence of a hypothetical instantaneous concentration jump.

Biochemical methods allow different steps of the enzymatic cycle of the calcium pump to be singled out, but cannot establish their electrogenicity. Conversely, the electrophysiological method based on the SSM allows the time dependence of the electrogenic events of the pump to be measured, but cannot ascribe them to well defined steps. Moreover, the time constants of the fastest processes cannot be resolved, since they are hidden by the rising phase of the current transient, which covers about 25 ms after the ATP concentration jump. In the present work it will be shown that, upon combining the available kinetic data provided by biochemical methods with reasonable assumptions as to the nature of the electrogenic steps, it is possible to fit the current transients calculated by numerical solution of the pertinent set of differential equations to the experimental current transients obtained by the SSM technique (including their rising section). This will permit us to gain further insight into the kinetics of the enzymatic cycle of Ca-ATPase and to verify that the rising section of the experimental current transients is due not only to the concentration jump being non-instantaneous, but also to some initial electrosilent steps.

After considering the kinetic scheme required to fit the current transients due to ATP concentration jumps, the change in the current transients following ATP concentration jumps in the presence of curcumin, an important inhibitor of carcinogenesis, will be examined [38]. Our results clearly show that curcumin reduces calcium transport by the calcium pump, while decreasing at the same time its rate of slippage [13,39].

2. Materials and methods

2.1. Chemicals

Calcium and magnesium chlorides and 3-morpholinopropane sulfonic acid (MOPS) were obtained from Merck at analytical grade. Adenosine-5′-triphosphate disodium salt (ATP, ~97%) and dithiothreitol (DTT, ≥99%) were purchased from Fluka. *n*-octadecanethiol (98%) from Aldrich was used without further purification. Ethylene glycol-bis[β-aminoethyl ether]-*N*, *N*, *N*', *N*'-tetraacetic acid (EGTA), calcimycin (calcium ionophore A23187) and curcumin were obtained from Sigma. The lipid solution contained diphytanoylphosphatidylcholine (Avanti Polar Lipids) and octadecylamine (puriss., Fluka) [60:1] and was prepared at a concentration of 1.5% (w/v) in *n*-decane (Merck) as described by Bamberg et al. [40].

Sarcoplasmic reticulum vesicles were obtained by extraction from the fast twitch hind leg muscle of a New Zealand white rabbit, followed by homogenization and differential centrifugation, as described by Eletr and Inesi [41]. The vesicles so obtained (light vesicles), derived from longitudinal SR membrane, contained only negligible amounts of the ryanodine receptor Ca^{2+} channel associated with junctional SR. The protein/lipid ratio was 1:1 and the total protein content was 22.4 mg/ml, of which about 50% consisting of Ca-ATPase.

2.2. The activation experiment

The vesicles were first adsorbed on an octadecanethiol/diphytanoylphosphatidylcholine mixed bilayer tethered to a gold electrode (namely the solid supported membrane, SSM) and were then chemically activated by a fast ATP concentration jump. A detailed description of the SSM, the experimental set-up and the solution exchange technique can be found in Ref. [34]. In all experiments two buffered solutions were employed, the non-activating and the activating solution. The non-activating solution contained 150 mM choline chloride, 25 mM MOPS (pH 7.0), 1 mM EGTA, 1 mM $MgCl_2$, 1.1 mM $CaCl_2$ ($[Ca^{2+}]_{free}$ = 100 μM) and 0.2 mM DTT. The activating solution had the same composition as the non-activating solution, plus 100 μM ATP. In the experiments with curcumin, this drug was added at the same concentration to both solutions from a 10 mM stock solution in ethanol. Free Ca^{2+} concentrations were calculated by the computer program WinMAXC 2.40 (Stanford University, Pacific Grove, CA — USA) [42].

Unless otherwise stated, 1 μM calcium ionophore A23187 was used to prevent formation of a Ca^{2+} concentration gradient across the SR vesicles [43]. In order to verify the reproducibility of the current transients generated within the same set of measurements on the same SSM, each single measurement of the set was repeated four to five times and then averaged to improve the signal-to-noise ratio. Average standard deviations were usually found to be no greater than ±5%.

For signal elaboration, charges were calculated by integrating the acquired current transients, while relaxation time constants were obtained by a multi-exponential fit to the current decreasing branch of the transient. In both cases the elaboration software Origin 7.0 (OriginLab Corporation, Nothampton, MA — USA) was used.

3. Results

A current transient induced at pH 7 by a 100 μM ATP concentration jump in the presence of 100 μM free Ca^{2+} and of the calcium ionophore A23187 is shown in Fig. 1. The normalized charge reported in Ref. [34] by numerical integration of the current transients recorded in the presence of both A23187 and the protonophore 1799 (1.25 μM) at different pH values, under

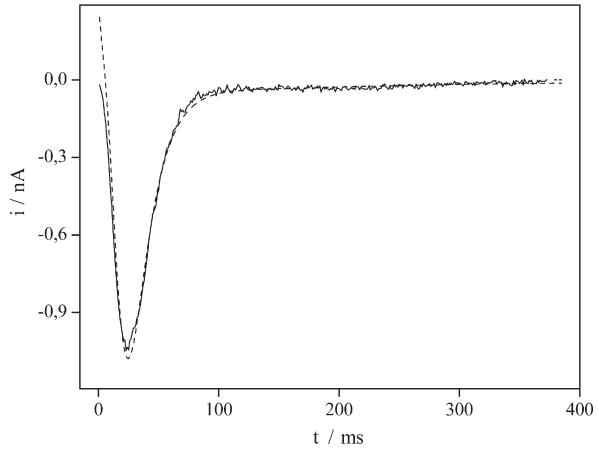

Fig. 1. A typical current transient following a 100 μM ATP concentration jump in the presence of 100 μM free Ca^{2+} at pH 7. The *dashed curve* was calculated as described in the text. The electrical parameters C_m, C_p and R_p employed for the fitting are 0.30 μF cm^{-2}, 3.9 μF cm^{-2} and 60 kΩ cm^2, respectively. The time t_{app} used to account for the ATP concentration jump being non-instantaneous (see Ref. [34]) is 140 ms.

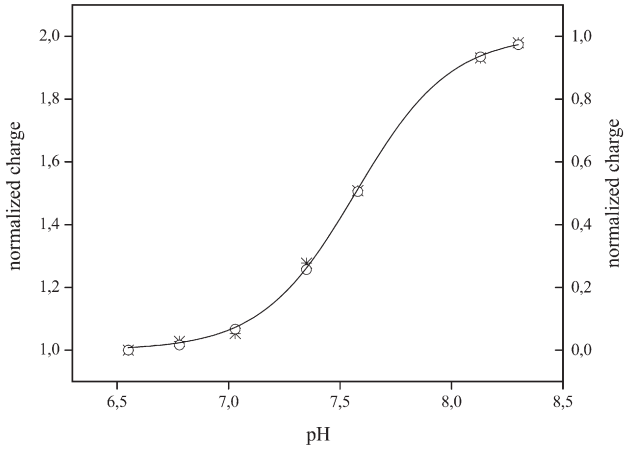

Fig. 2. Translocated charge following 100 μM ATP concentration jumps in the presence of 100 μM free Ca^{2+} as a function of pH. The charge is normalized to unity at pH 6.55 on the left-hand vertical axis. The right-hand vertical axis is used for the fitting to Eq. (4). *Asterisks* are experimental data (from Ref. [34]), while *open circles* are obtained from the simulation for a K value of 1.4×10^{15} M^{-2}. The *solid curve* is the best fit of the Hill function to the normalized charge, yielding $K_{0.5}=1.8\times10^{-8}$ M ($pK_{0.5}=7.7$) and a Hill coefficient n of 2.0 ± 0.3. The $K_{0.5}$ value corresponds to a binding constant, K_b, of 3.1×10^{15} M^{-2}.

otherwise identical conditions, is plotted against pH in Fig. 2 (*asterisks*).

The presence of curcumin markedly affects the shape and the magnitude of the current transients recorded under the same experimental conditions as in Fig. 1. Fig. 3 reports a number of current transients in the presence of different curcumin concentrations. A progressive increase in the curcumin concentration causes a modest increase both in the peak current and in the charge under the current transient up to 5 μM, followed by their decrease at higher concentrations, as shown in Fig. 4. An analogous dependence upon curcumin concentration was reported by Sumbilla et al. [39] for Ca^{2+} transport in the presence of ATP. Fitting a bi-exponential function to the current decreasing branch of the transients, with the origin of the time axis placed at the current peak, yields two relaxation time constants. The dependence of the shortest time constant, τ_1, upon the curcumin concentration parallels those of the charge and of the

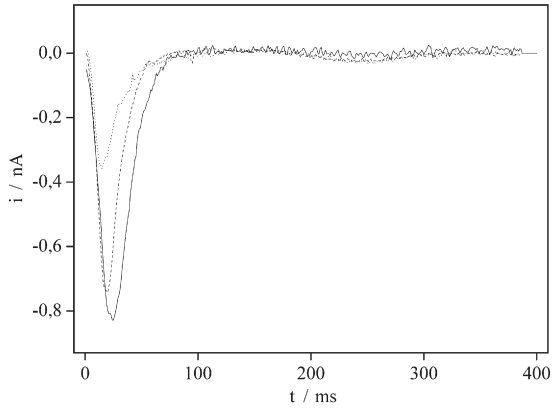

Fig. 3. Experimental current transients following 100 μM ATP concentration jumps at pH 7 in the presence of 100 μM free Ca^{2+} and of 0 (*solid line*), 15 μM (*dashed line*) and 20 μM (*dotted line*) curcumin.

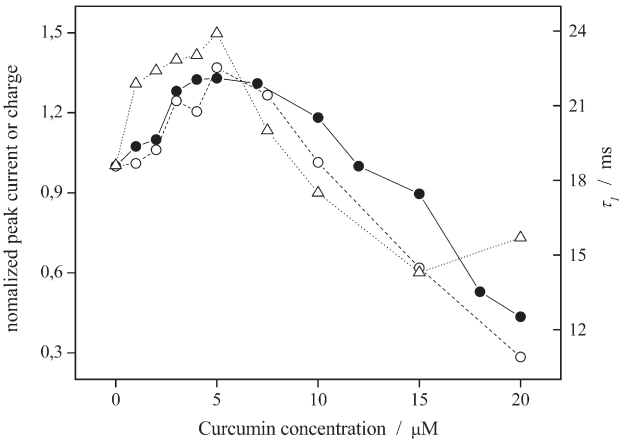

Fig. 4. Dependence of peak current (● and *solid curve*), translocated charge (○ and *dashed curve*) and decay time constant τ_1 (△ and *dotted curve*) upon curcumin concentration, as obtained from 100 μM ATP concentration jumps in the presence of 100 μM free Ca^{2+} at pH 7. Peak current and charge are normalized to the corresponding values in the absence of curcumin.

peak current, as shown in Fig. 4. The longer time constant is greater than 200 ms and is practically equal to the product of the capacity by the resistance of the vesicular membrane (see Ref. [34]); it does not depend on the pump activity and its high value does not affect the estimate of τ_1.

It should be noted that in the above concentration jump experiments potassium ion was absent. On the other hand, Sumbilla et al. [39] and Logan-Smith et al. [13] used a high concentration of K^+ in their biochemical measurements. To verify the effect of curcumin on Ca-ATPase in the presence of K^+, 100 μM ATP concentration jumps were performed with the SSM technique in the presence of 80 mM KCl and different curcumin concentrations. The dependence of the current transients on curcumin concentration observed in the presence of potassium ions is in agreement with that reported in Fig. 4 (*data not shown*).

4. Discussion

4.1. Electrogenic steps of the SR Ca-ATPase enzymatic cycle

A detailed sequence of the steps of the enzymatic cycle of Ca-ATPase, with the corresponding forward and backward rate constants at physiological pH, was provided by Inesi and coworkers on the basis of a number of biochemical measurements [18,39]. In this sequence the protonation and deprotonation steps are not reported. However, they can be readily included on the basis of the consideration that these steps are normally regarded as sufficiently fast as to be considered in quasi-equilibrium, to a good approximation. In other words, if the steps of the sequence reported in Ref. [39] are immediately followed by a protonation or deprotonation step in quasi-equilibrium, their rate constants incorporate the equilibrium constant of the latter step. Moreover, the sequence in Ref. [39] does not include explicitly a step involving the passage from the E_2 to the E_1 conformation.

The pH dependence of the charge moved by Ca-ATPase following Ca^{2+} concentration jumps in the absence of ATP, as

measured by the SSM technique over the pH range from 6 to 8.3, indicates unequivocally that the calcium pump in the E_1 conformation is deprotonated at pH 7 [36]. On the other hand, the pH dependence of the charge translocated by Ca-ATPase following ATP concentration jumps in the presence of Ca^{2+} indicates that the E_2 conformation at pH 7 is present substantially in the H_2E_2 form [34]. In particular, in view of the results of electrostatic calculations [44,45], the most probable candidates for deprotonation at pH 7 in the E_1 state are Glu-771 and Asp-800, thus favoring Ca^{2+} binding. It is then likely that these two residues acquire protons upon Ca^{2+} release following the conformational change from E_1 to E_2. Conversely, Glu-309 and Glu-908 are likely to retain their protons through the whole cycle, because of their involvement in hydrogen binding and stabilization of the Ca^{2+}-bound conformation. With this in mind, the sequence in Ref. [39] is complemented as shown in Scheme 1.

To fit this scheme to the experimental current transient in Fig. 1, the charge associated to each step must first be established. For this purpose, the following reasonable assumptions, supported by several pieces of experimental evidence, are made:

(1) The charge movements confined to the extramembrane domains of the pump are entirely screened by the aqueous medium, and the steps involving these movements must, therefore, be regarded as electrosilent. This applies, say, to ATP and ADP binding and to phosphorylation and dephosphorylation steps [22].
(2) Conformational changes, which may involve movements of cytoplasmic domains of the pump or rotations of the transmembrane α-helices, are also regarded as substantially electrosilent. Fluorescence measurements with styryl dyes support this assumption [22,24–26]. This confines the electrogenicity only to the steps involving H^+ or Ca^{2+} movements within the transmembrane portion of the pump.
(3) The transmembrane domain of the pump is assumed to be homogeneous from a dielectric point of view. In other words, no wide water-filled openings (vestibules) with the dielectric constant, $\varepsilon = 80$, of bulk water are considered to be present in the transmembrane domain of the calcium pump. This assumption is supported by the recently published crystal structures of Ca-ATPase in four different states, Ca_2E_1, $ATP{\cdot}E_1$, $P{-}E_2$ and E_2-thapsigargin [46–52], which do not show large vestibules in the transmembrane domain. Thus, recent continuum electrostatic calculations [45], which are based on a 2.4-Å-resolution crystal structure of Ca-ATPase and account for the presence of water and phospholipid molecules within narrow clefts in the transmembrane domain, ascribe a dielectric constant of 4 to this domain.
(4) The dielectric coefficient of a step is defined as the fraction of the thickness of the membrane, assumed to be a homogeneous dielectric film, across which the charge is moved during the given step, times the moved charge expressed in electronic units. At pH 7.0, the dielectric coefficient of a step involving the passage of a proton from the luminal side of the pump to its binding site will be assumed to be equal to −0.67. Accordingly, the dielectric coefficient of a Ca^{2+} ion moving in the opposite direction will be equated to +1.34 [34]. Analogously, the dielectric coefficient of a step involving the passage of a proton from its binding site to the cytoplasmic side will be set equal to −0.33, while that of a Ca^{2+} moving in the opposite direction will be equated to +0.67. This assumption is based on the known Ca_2E_1 structure [43],

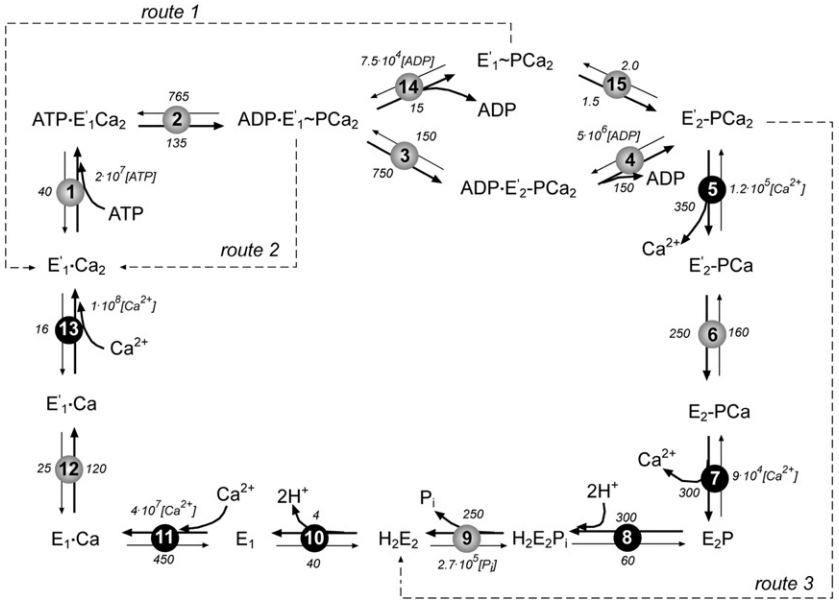

Scheme 1. Enzymatic cycle of SR Ca-ATPase, at pH 7, after Sumbilla et al. [39], complemented as explained in the text. Numbering starts from the ATP concentration jump. Forward and backward rate constants for each step are reported. Gray circles denote electrosilent steps, black circles electrogenic steps. Dotted lines indicate three different routes for slippage reported in Ref. [55] (*route 1*), Ref. [39] (*route 2*) and Refs. [13,56] (*route 3*).

where the Ca^{2+} binding moiety is located inside the membrane domain, at about 30–40% of the membrane thickness from the cytoplasmic side. Moreover, in the P–E_2 conformation the transmembrane segments that form the ion binding site are not dramatically shifted relative to their position in the E_1 conformation [44]. Finally, the protons involved in Ca^{2+} translocation are expected to be taken up by, or released from, the residues that coordinate the Ca^{2+} ions, thereby occupying the same location as calcium within the transmembrane domain.

The current transient based on Scheme 1 was calculated by solving the system of fourteen differential equations obtained by equating the time derivative of the mole fraction of each state of the pump to the sum of the rates that yield the given state minus those that consume it, according to the usual procedure [37,53]. To obtain the capacitive current I that flows along the external circuit and yields the current transient, a further differential equation was added to the above equations. This was derived from the analysis of an equivalent circuit reported in Fig. 13 of Ref. [34], which is used to simulate the SSM. It consists of an R_pC_p mesh, simulating the vesicular membrane, with in parallel a current source simulating the ion pump, and with in series a further R_mC_m mesh simulating the mixed thiol/lipid bilayer. The analysis of this equivalent circuit yields the two differential equations [34]:

$$I = I_p S(t) + C_p \frac{dv_p}{dt} + \frac{v_p}{R_p} \quad \text{(a)}; \tag{1}$$

$$I = \frac{v_m}{R_m} + C_m \frac{dv_m}{dt} \quad \text{(b)}$$

Here, I_p is the pump current, v_p and v_m are the potential differences across the vesicular membrane and across the mixed bilayer, respectively, while $S(t)$ is a step function. In practice, R_m is so high that the first term in Eq. (1b) can be neglected to a good approximation. Noting that at constant applied potential E we have: $dv_m/dt = -dv_p/dt$, combining this equation with Eq. (1a and b) yields the fifteenth differential equation:

$$\frac{dv_p}{dt} = -\frac{I_p}{C_m + C_p} - \frac{v_p}{R_p(C_p + C_m)}. \tag{2}$$

The resulting system of fifteen differential equations was solved by the fourth-order Runge–Kutta method. After obtaining the mole fractions of the fourteen states of the pump and v_p as a function of time, the pump current I_p was obtained by summing the rates of all fifteen steps, each rate being multiplied by the corresponding dielectric coefficient. The current I was then obtained from the equation:

$$I = -C_m dv_p/dt. \tag{3}$$

The best fit, represented by the dashed curve in Fig. 1, was obtained by using all the rate constants reported by Sumbilla et al. [39], except for the forward rate constant of the $E_2P \Leftrightarrow H_2E_2P_i$ step, which was set equal to 300 s^{-1} at pH 7.0, instead of 60 s^{-1}. Incidentally, this rate constant embodies the equilibrium constant for the overall protonation reaction $E_2P + 2H^+ \Leftrightarrow H_2E_2P$ (or $E_2P_i + 2H^+ \Leftrightarrow H_2E_2P_i$) at pH 7. The $H_2E_2 \Leftrightarrow E_1 + 2H^+$ step (step 10 in Scheme 1), which embodies the equilibrium constant for the overall deprotonation reaction $H_2E_1 \Leftrightarrow E_1 + 2H^+$, was not explicitly included in the reaction sequence by Sumbilla et al. [39]. The best fit was obtained by ascribing a forward and a backward constant of 4 and 40 s^{-1}, respectively, to this step. For each simulation, the electrical parameters C_m, C_p and R_p were adjusted so as to obtain the best fit of the scheme to the experimental current transient for an ATP concentration jump in the absence of curcumin; C_m, C_p and R_p were selected in the range 0.2–0.3 μF/cm^2, 2.5–3.9 μF/cm^2, and 45–85 kΩ cm^2, respectively. In particular, the value of R_p is in good agreement with that reported in Ref. [34]. Even relatively small changes in the rate constants involving the time range covered by the current transients have an appreciable effect on the shape and height of the corresponding calculated transients (*data not shown*).

The charge moved in the presence of 100 μM free Ca^{2+} following a 100 μM ATP concentration jump yields a sigmoidal curve when plotted against pH (see Fig. 2), practically doubling in passing from pH 7 to pH 8.3. This increase in the net translocated charge with an increase in pH is due to the progressive decrease in the countertransport of protons from the lumen to the cytoplasm until, at pH 8.3, no proton countertransport takes place. This behavior is to be ascribed to residues of the Ca^{2+} binding site which, when exposed to the luminal side of the pump, release two Ca^{2+} ions and take up a number of protons that depends on their pK. In particular, at pH 7, two protons are taken up by these residues and translocated to the cytoplasm. The sigmoidal curve in Fig. 2, measured from its foot and normalized to unity (see the right-hand vertical axis), is due to the gradual passage of the E_2 conformation from the H_2E_2P to the E_2P form, and is directly related to the protonation constants $K_1 = [HE_2P]/([E_2P][H^+])$ and $K_2 = [H_2E_2P]/([HE_2P][H^+])$, according to the expression:

$$\frac{[E_2P]}{[E_2P] + [HE_2P] + [H_2E_2P]} = \frac{1}{1 + K_1[H^+] + K_1K_2[H^+]^2}. \tag{4}$$

In fact, this expression passes from the zero to the unit value with an increase in pH, over the pH range investigated. A fit of Eq. (4) to the sigmoidal curve of Fig. 2 shows that K_2 is much greater than K_1, such that only the overall protonation equilibrium $K = K_1K_2 = [H_2E_2P]/([E_2P][H^+]^2)$ is measurable. In other words, the intrinsic affinity of the proton for the second protonation site is much greater than that for the first site, denoting maximum cooperativity. This is clearly shown by the best fit of the Hill function to the experimental plot (solid curve in Fig. 2). This fit yields a $K_{0.5}$ value of 1.8×10^{-8} M (p$K_{0.5}$ = 7.7) and a Hill coefficient n of 2.0 ± 0.3, with $K_{0.5}$ corresponding to a binding constant, K_b, of 3.1×10^{15} M^{-2}. The current transients at the pH values corresponding to the experimental points in Fig. 2 were calculated as described above (see Fig. 5). In this connection, the progressive change in proton countertransport was accounted for by multiplying the dielectric

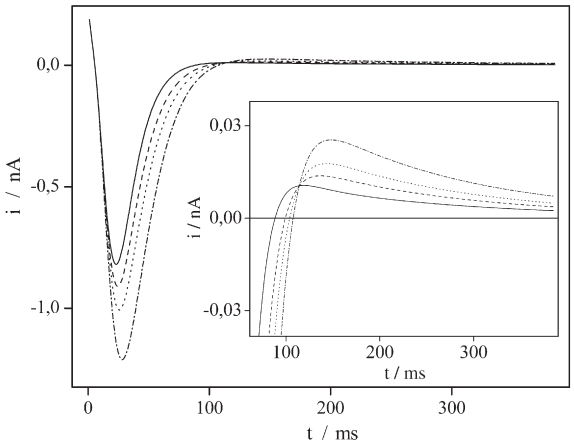

Fig. 5. Simulated current transients for 100 μM ATP concentration jumps in the presence of 100 μM free Ca^{2+} at different pH values: 6.55 (*solid line*), 7.35 (*dashed line*), 7.58 (*dotted line*), 8.30 (*dashed–dotted line*). The inset shows the region of the overshoot.

coefficients of the $E_2P+2H^+ \Leftrightarrow H_2E_2P_i$ and $H_2E_2 \Leftrightarrow E_1+2H^+$ steps by the factor:

$$\frac{[H_2E_2P]}{[E_2P]+[H_2E_2P]} = \frac{K[H^+]^2}{1+K[H^+]^2}. \quad (5)$$

This amounts to considering that the $E_2P+2H^+ \Leftrightarrow H_2E_2P_i$ step runs in parallel with an $E_2P \Leftrightarrow E_2P_i$ step, and that the $H_2E_2 \Leftrightarrow E_1+2H^+$ step runs in parallel with a $H_2E_2 \Leftrightarrow H_2E_1$ step, the relative weight of the parallel steps depending on pH. The $E_2P \Leftrightarrow E_2P_i$ and $H_2E_2 \Leftrightarrow H_2E_1$ steps do not contribute to proton movement, while the $E_2P+2H^+ \Leftrightarrow H_2E_2P_i$ and $H_2E_2 \Leftrightarrow E_1+2H^+$ steps do. The charge obtained by numerical integration of the current transients so calculated was plotted against pH (open circles in Fig. 2). The best fit to the experimental charge vs. pH plot in Fig. 2 was obtained for $K=K_1K_2=1.4\times10^{15}$ M^{-2}. It should be noted that this K value, which is obtained by correctly calculating the effect of the pH dependence of the protonation state of the E_2 conformation on the experimental charge, is slightly different from the $K_{0.5}$ value obtained by directly applying the Hill function to the charge vs. pH plot. The calculated curves show an increasing overshoot with an increase in pH (see Fig. 5), in qualitative agreement with the experimental behavior (compare Fig. 7 of Ref. [34]).

It is interesting to compare the equilibrium and kinetic data for the conformational transition from the E_1 to the E_2 states, as obtained at pH 7 from the fit of the current transient in Fig. 1, with those obtained by Henderson et al. [14,15] in the absence of ATP and of Ca^{2+} by using 4-nitrobenzo-2-oxa-1,3-diazole (NBD) as a fluorescent probe sensitive to this conformational change. In making this comparison, one must consider that these authors extract their equilibrium and kinetic parameters from their fluorescence measurements, upon assuming that both E_1 and E_2 are present exclusively in the deprotonated or monoprotonated forms over the whole pH range from 6 to 8.5. On the other hand, our measurements of the pH dependence of charge movements, following Ca^{2+} concentration jumps in the absence of ATP and ATP concentration jumps in the presence of Ca^{2+}, show unequivocally that, at pH 7, E_2 is almost completely present in the fully protonated form, H_2E_2 [34,36]. Among other things, this protonation state allows a straightforward interpretation of the countertransport of two protons per enzymatic cycle of the calcium pump at physiological pH. Leaving this difference in the protonation states of E_2 aside, the equilibrium constants for the $E_1 \Leftrightarrow E_1H$ and $E_2 \Leftrightarrow E_2H$ steps, $K_{1,p}=5\times10^5$ M^{-1} and $K_{2,p}=3\times10^8$ M^{-1} respectively, estimated by Henderson et al. [14], indicate that, at pH 7, the E_1 conformation is fully deprotonated and the E_2 conformation is fully protonated, in agreement with our results. Moreover, the ratio of the overall concentration of E_1 to that of E_2 at equilibrium, $([E_1]+[E_1H])/([E_2]+[E_2H])$, as estimated at pH 7 from the above $K_{1,p}$ and $K_{2,p}$ equilibrium constants and from the equilibrium constant, 4, for the $E_1 \Leftrightarrow E_2$ step reported by Henderson et al. [14], amounts to 0.13, in good agreement with the $[E_1]/[H_2E_2]$ ratio of 0.1 estimated at pH 7 from the forward and backward rate constants of the $H_2E_2 \Leftrightarrow E_1$ step in Scheme 1. In addition, the pH at which the E_2 and E_1 conformations assume equal concentrations, independent of their protonation states, amounts to about 7.5 according to Henderson's measurements (see Fig. 1 of Ref. [14]). This pH value compares very favorably with that of 7.6, estimated from ATP concentration jumps in the presence of Ca^{2+} (see Fig. 2). Finally, the "overall" forward rate constant of the $E_2 \rightarrow E_1$ transition, as estimated from the $K_{1,p}$ and $K_{2,p}$ equilibrium constants and from the forward rate constants of the $E_2 \rightarrow E_1$ and $HE_2 \rightarrow HE_1$ steps, 80 and 2 s^{-1} respectively, as reported by Henderson et al. [15], amounts to 4.5 s^{-1} at pH 7; this value agrees satisfactorily with the value of 4 s^{-1} in Scheme 1 (step 10).

The above results indicate that, under non-steady state conditions, the slowest step of the enzymatic cycle of the pump is an electrosilent relaxation from the E_2 to the E_1 conformation (probably, a $H_2E_2 \rightarrow H_2E_1$ step followed by a rapid release of two protons, at pH 7). The agreement of our rate and equilibrium constants with those by Henderson et al. [14,15] also points out that the rate of this step is independent of the presence of Ca^{2+} or ATP. That the transition from the E_2 to the E_1 configuration is the slowest step of the whole cycle was first reported by Scofano et al. [54], at ATP concentrations below 50 μM. This conclusion is consistent with the large rearrangements occurring between the Ca_2E_1 state and the thapsigargin-stabilized E_2 state, as results from these two crystal structures [46,47]. Similar conclusions were recently drawn by Peinelt and Apell [25], who estimate the rate of the $H_2E_2 \rightarrow H_2E_1$ step at 0.8 s^{-1}. However, these authors propose that a change between two different conformations of P–E_2 (P–E_2* → P–E_2) may be even slightly slower. The relatively long time required for Ca-ATPase to complete a single cycle (about 250 ms from our measurements, about 1 s from Peinelt and Apell's fluorescence measurements) is in apparent contrast with the short time (50 ms or less) during which a muscle relaxation process takes place. However, the high density of calcium pumps in the SR allows the Ca^{2+} concentration in the cytoplasm to pass from 10 to 0.1 μM by Ca^{2+} binding in the E_1 state in a single turnover of the pumps [25]. Now, this binding takes place in less than 50 ms.

4.2. Effect of curcumin

We will now examine the peculiar behavior of curcumin, an important inhibitor of carcinogenesis [38]. This drug is reported to inhibit the ATPase activity of Ca-ATPase, while reducing at the same time its rate of slippage [13,39]. Thus, according to Sumbilla's biochemical measurements, a progressive increase in curcumin concentration causes calcium transport first to increase, attaining maximum at 5 μM curcumin, and then to decrease continuously, remaining higher than in the absence of curcumin only up to 10 μM. On the other hand, the ATPase activity increases only slightly up to a 2 μM concentration and then decreases continuously [39]. Our SSM measurements of Ca^{2+} translocation following ATP concentration jumps confirm such an effect of curcumin on Ca^{2+} transport (see Fig. 4). In the absence of curcumin, the slippage, namely the ATP hydrolysis without Ca^{2+} translocation induced by the pump, increases with an increase in the concentration of ADP or in that of luminal Ca^{2+}. Three possible routes for slippage are represented by dashed lines in Scheme 1. Route 1 was proposed by de Meis [55], route 2 by Sumbilla et al. [39], and route 3 by Dalton et al. [56] and by Logan Smith et al. [13].

To investigate whether the effect of curcumin on Ca^{2+} transport is influenced by adding ADP to the buffer solution, 100 μM ATP concentration jumps have been carried out in the presence of ADP and different curcumin concentrations. Fig. 6 shows the translocated charge in the presence of 0, 4 and 15 μM curcumin and in the presence of 10 (panel A) and 100 μM (panel B) ADP. All charges were normalized to that recorded in the absence of both ADP and curcumin, taken as reference and denoted by an asterisk. It is apparent that curcumin has practically no effect in the presence of both ADP concentrations. The notable decrease in charge upon addition of 100 μM ADP (panel B) is to be ascribed to reversal of the enzymatic cycle and to uncoupled Ca^{2+} efflux [55]. These results indicate that curcumin inhibits Ca-ATPase by competing with ADP. However, it is unlikely that curcumin may compete for the nucleotide binding site by mimicking ADP, in view of the hydrophobic nature of this drug. It is more probable that it acts as a competitive inhibitor by inducing a conformational change that prevents ADP from binding.

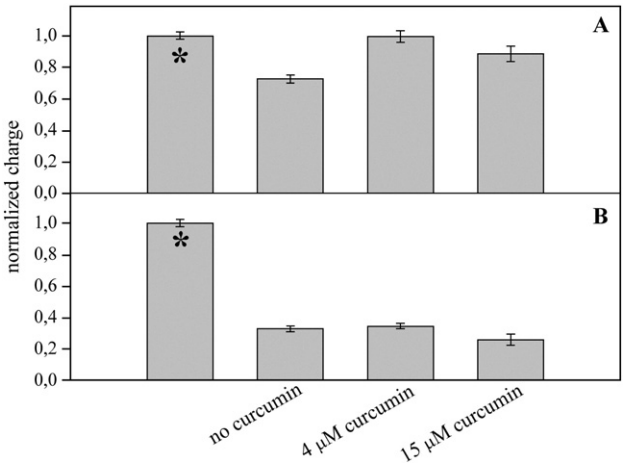

Fig. 6. Translocated charge following 100 μM ATP concentration jumps in the presence of 0, 4 and 15 μM curcumin and in the presence of 10 (A) or 100 μM (B) ADP. All charges were normalized to that recorded in the absence of both ADP and curcumin, taken as reference and denoted by an asterisk in both panels.

A clue to the steps that may be affected by curcumin is provided by the observation that the relaxation time, τ, in Fig. 4 varies in parallel with the translocated charge, as the curcumin concentration is increased. In other words, an increase in the corresponding rate, $1/\tau$, is accompanied by a decrease in Ca^{2+} translocation, and vice versa. This is an unusual behavior, and suggests an effect of curcumin on the rates of branched reactions in the enzymatic cycle of the calcium pump. In fact, an increase in the rate of an unbranched step of the enzymatic cycle is expected to increase the rate of Ca^{2+} translocation, and vice versa. Thus, for instance, a progressive increase in the concentration of cyclopiazonic acid, which inhibits the Ca-ATPase activity [57], causes both a decrease in the translocated charge and an abrupt increase in the relaxation time τ obtained from the mono-exponential decay of the current transient (*data not shown*).

In conclusion, the forward and backward rate constants of the various steps of the enzymatic cycle of the calcium pump provided by Sumbilla et al. [39], combined with suitable dielectric coefficients of the electrogenic steps and with a more detailed kinetic analysis of the E_2/E_1 conformational change, provide a satisfactory interpretation of the electrophysiological response of the calcium pump to ATP concentration jumps in the presence of Ca^{2+}. The alteration of this response induced by curcumin, which reduces calcium transport by Ca-ATPase while decreasing its rate of slippage, has been examined. Starting from Scheme 1, it would be interesting to verify if the modulating effect of curcumin on the calcium pump may be reasonably explained by an alteration of the kinetics of some of these steps.

Acknowledgements

The authors wish to thank Prof. Giuseppe Inesi (California Pacific Medical Center Research Institute, San Francisco, California, U.S.A.) for providing them with SR native vesicles containing Ca-ATPase. The financial support of Ente Cassa di Risparmio di Firenze, through the PROMELAB project, and of MIUR (Italian Ministry of Education, University and Research), through the grant PRIN 2004 035330, are gratefully acknowledged.

References

[1] D.L. Stokes, N.M. Green, Structure and function of the calcium pump, Annu. Rev. Biophys. Biomol. Struct. 32 (2003) 445–468.
[2] G. Inesi, C. Toyoshima, Catalytic and transport mechanism of the sarco-(endo)plasmic reticulum Ca^{2+}-ATPase (SERCA), in: M. Futai, Y. Wada, J.H. Kaplan (Eds.), Handbook of ATPases, Wiley-VCH Verlag GmbH & Co. KGaA, Weinheim, Germany, 2004, pp. 63–87.
[3] J.V. Møller, P. Nissen, T.L.-M. Sørensen, M. le Maire, Transport mechanism of the sarcoplasmic reticulum Ca^{2+}-ATPase pump, Curr. Opin. Struct. Biol. 15 (2005) 387–393.
[4] S. Yamada, N. Ikemoto, Reaction mechanism of calcium-ATPase of sarcoplasmic reticulum, J. Biol. Chem. 255 (1980) 3108–3119.
[5] T. Menguy, F. Corre, L. Bouneau, S. Deschamps, J.V. Møller, P. Champeil, M. le Maire, P. Falson, The cytoplasmic loop located between transmembrane

segments 6 and 7 controls activation by Ca^{2+} of sarcoplasmic reticulum Ca^{2+}-ATPase, J. Biol. Chem. 273 (1998) 20134–20143.
[6] S. Hua, H. Ma, D. Lewis, G. Inesi, C. Toyoshima, Functional role of "N" (nucleotide) and "P" (phosphorylation) domain interactions in the sarcoplasmic reticulum (SERCA) ATPase, Biochemistry 41 (2002) 2264–2272.
[7] G. Inesi, Z. Zhang, D. Lewis, Cooperative setting for long-range linkage of Ca^{2+} binding and ATP synthesis in the Ca^{2+}-ATPase, Biophys. J. 83 (2002) 2327–2332.
[8] G. Inesi, M. Kurzmack, C. Coan, D.E. Lewis, Cooperative calcium binding and ATPase activation in sarcoplasmic reticulum vesicles, J. Biol. Chem. 255 (1980) 3025–3031.
[9] V. Forge, E. Mintz, F. Guillain, Ca^{2+} binding to sarcoplasmic reticulum ATPase revisited. I. Mechanism of affinity and cooperativity modulation by H^+ and Mg^{2+}, J. Biol. Chem. 268 (1993) 10953–10960.
[10] V. Forge, E. Mintz, F. Guillain, Ca^{2+} binding to sarcoplasmic reticulum ATPase revisited. II. Equilibrium and kinetic evidence for a two-route mechanism, J. Biol. Chem. 268 (1993) 10961–10968.
[11] J.V. Møller, G. Lenoir, C. Merchand, C. Montigny, M. le Maire, C. Toyoshima, B.S. Juul, P. Champeil, Calcium transport by sarcoplasmic reticulum Ca^{2+}-ATPase, J. Biol. Chem. 277 (2002) 38647–38659.
[12] P. Champeil, F. Henao, J.J. Lacapere, D.B. McIntosch, A remarkably stable phosphorylated form of Ca^{2+}-ATPase prepared from Ca^{2+}-loaded and fluorescein isothiocyanate-labeled sarcoplasmic reticulum vesicles, J. Biol. Chem. 276 (2001) 5795–5803.
[13] M.J. Logan-Smith, P.J. Lockyer, J.M. East, A.G. Lee, Curcumin, a molecule that inhibits the Ca^{2+}-ATPase of sarcoplasmic reticulum but increases the rate of accumulation of Ca^{2+}, J. Biol. Chem. 276 (2001) 46905–46911.
[14] I.M.J. Henderson, Y.M. Khan, J.M. East, A.G. Lee, Binding of Ca^{2+} to the (Ca^{2+}–Mg^{2+})-ATPase of sarcoplasmic reticulum: equilibrium studies, Biochem. J. 297 (1994) 615–624.
[15] I.M.J. Henderson, A.P. Starling, M. Wictome, J.M. East, A.G. Lee, Binding of Ca^{2+} to the (Ca^{2+}–Mg^{2+})-ATPase of sarcoplasmic reticulum: kinetic studies, Biochem. J. 297 (1994) 625–636.
[16] J.P. Froehlich, P.F. Heller, Transient-state kinetics of the ADP-insensitive phosphoenzyme in sarcoplasmic reticulum: implications for transient-state calcium translocation, Biochemistry 24 (1985) 126–136.
[17] J.A. Teruel, M. Kurzmack, G. Inesi, Kinetic and thermodynamic control of ATP synthesis by sarcoplasmic reticulum adenosine-triphosphatase, J. Biol. Chem. 262 (1987) 13055–13060.
[18] G. Inesi, M. Kurzmack, D. Lewis, Kinetic and equilibrium characterization of an energy-transducing enzyme and its partial reactions, Methods Enzymol. 157 (1988) 154–190.
[19] G. Inesi, L. de Meis, Regulation of steady state filling in sarcoplasmic reticulum. Roles of back-inhibition, leakage, and slippage of the calcium pump, J. Biol. Chem. 264 (1989) 5929–5936.
[20] T.L. Sørensen, Y. Dupont, B. Vilsen, J.P. Andersen, Fast kinetic analysis of conformational changes in mutants of the Ca^{2+}-ATPase of sarcoplasmic reticulum, J. Biol. Chem. 275 (2000) 5400–5408.
[21] G.L. Alonso, D.A. Gonzalez, D. Takara, M.A. Ostuni, G.A. Sanchez, Kinetic analysis of a model of the sarcoplasmic reticulum Ca-ATPase, with variable stoichiometry, which enhances the amount and the rate of Ca transport, J. Theor. Biol. 208 (2001) 251–260.
[22] C. Butscher, M. Roudna, H.J. Apell, Electrogenic partial reactions of the SR-Ca-ATPase investigated by a fluorescence method, J. Membr. Biol. 168 (1999) 169–181.
[23] M. Pedersen, M. Roudna, S. Beutner, M. Birmes, B. Reifers, H.-D. Martin, H.-J. Apell, Detection of charge movements in ion pumps by a family of styryl dyes, J. Membr. Biol 185 (2001) 221–236.
[24] C. Peinelt, H.-J. Apell, Kinetics of the Ca^{2+}, H^+, and Mg^{2+} interaction with the ion-binding sites of the SR Ca-ATPase, Biophys. J. 82 (2002) 170–181.
[25] C. Peinelt, H.-J. Apell, Time-resolved charge movements in the sarcoplasmatic reticulum Ca-ATPase, Biophys. J. 86 (2004) 815–824.
[26] C. Peinelt, H.-J. Apell, Kinetics of Ca^{2+} binding to the SR Ca-ATPase in the E_1 state, Biophys. J. 89 (2005) 2427–2433.
[27] J. Pintschovius, K. Fendler, Charge translocation by the Na^+/K^+-ATPase investigated on solid supported membranes: rapid solution exchange with a new technique, Biophys. J. 76 (1999) 814–826.
[28] J. Pintschovius, E. Bamberg, K. Fendler, Charge translocation by the Na^+/K^+-ATPase investigated on solid supported membranes: cytoplasmic cation binding and release, Biophys. J. 76 (1999) 827–836.
[29] K. Meyer-Lipp, C. Ganea, T. Pourcher, G. Leblanc, K. Fendler, Sugar binding induced charge translocation in the melibiose permease from *Escherichia coli*, Biochemistry 43 (2004) 12606–12613.
[30] A. Zhou, A. Wozniak, K. Meyer-Lipp, M. Nietschke, H. Jung, K. Fendler, Charge translocation during cosubstrate binding in the Na^+/proline transporter of *E. coli*, J. Mol. Biol. 343 (2004) 931–942.
[31] D. Zuber, R. Krause, M. Venturi, E. Padan, E. Bamberg, K. Fendler, Kinetics of charge translocation in the passive downhill uptake mode of the Na^+/H^+ antiporter NhaA of *Escherichia coli*, Biochim. Biophys. Acta 1709 (2005) 240–250.
[32] K. Meyer-Lipp, N. Sery, C. Ganea, C. Basquin, K. Fendler, G. Leblanc, The inner interhelix loop 4–5 of the melibiose permease from *Escherichia coli* takes part in conformational changes after sugar binding, J. Biol. Chem. 281 (2006) 25882–25892.
[33] F. Tadini-Buoninsegni, P. Nassi, C. Nediani, A. Dolfi, R. Guidelli, Investigation of Na^+,K^+-ATPase on a solid supported membrane: the role of acylphosphatase on the ion transport mechanism, Biochim. Biophys. Acta 1611 (2003) 70–80.
[34] F. Tadini-Buoninsegni, G. Bartolommei, M.R. Moncelli, G. Inesi, R. Guidelli, Time-resolved charge translocation by sarcoplasmic reticulum Ca-ATPase measured on a solid supported membrane, Biophys. J. 86 (2004) 3671–3686.
[35] G. Bartolommei, F. Tadini-Buoninsegni, S. Hua, M.R. Moncelli, G. Inesi, R. Guidelli, Clotrimazole inhibits the Ca^{2+}-ATPase (SERCA) by interfering with Ca^{2+} binding and favoring the E2 conformation, J. Biol. Chem. 281 (2006) 9547–9551.
[36] F. Tadini-Buoninsegni, G. Bartolommei, M.R. Moncelli, R. Guidelli, G. Inesi, Pre-steady state electrogenic events of Ca^{2+}/H^+ exchange and transport by the Ca^{2+}-ATPase, J. Biol. Chem. 281 (2006) 37720–37727.
[37] P. Läuger, Electrogenic Ion Pumps, Sinauer Associates Inc., Sunderland, MA, USA, 1991.
[38] M.M. Manson, K.A. Holloway, L.M. Howells, E.A. Hudson, S.M. Plummer, M.S. Squires, S.A. Prigent, Modulation of signal-transduction pathways by chemopreventive agents, Biochem. Soc. Trans. 28 (2000) 7–12.
[39] C. Sumbilla, D. Lewis, T. Hammerschmidt, G. Inesi, The slippage of the Ca^{2+} pump and its control by anions and curcumin in skeletal and cardiac sarcoplasmic reticulum, J. Biol. Chem. 277 (2002) 13900–13906.
[40] E. Bamberg, H.J. Apell, N.A. Dencher, W. Sperling, H. Stieve, P. Läuger, Photocurrents generated by bacteriorhodopsin on planar bilayer membranes, Biophys. Struct. Mech. 5 (1979) 277–292.
[41] S. Eletr, G. Inesi, Phospholipid orientation in sarcoplasmic membranes: spin-label ESR and proton MNR studies, Biochim. Biophys. Acta 282 (1972) 174–179.
[42] D.M. Bers, C.W. Patton, R. Nuccitelli, A practical guide to the preparation of Ca^{2+} buffers, in: R. Nuccitelli (Ed.), Methods in Cell Biology, a Practical Guide to the Study of Calcium in Living Cells, vol. 40, Academic Press, 1994.
[43] K. Hartung, J.P. Froehlich, K. Fendler, Time-resolved charge translocation by the Ca-ATPase from sarcoplamic reticulum after an ATP concentration jump, Biophys. J. 72 (1997) 2503–2514.
[44] Y. Sugita, N. Miyashita, M. Ikeguchi, A. Kidera, C. Toyoshima, Protonation of the acidic residues in the transmembrane cation-binding sites of the Ca^{2+} pump, J. Am. Chem. Soc. 127 (2005) 6150–6151.
[45] K. Obara, N. Miyashita, C. Xu, I. Toyoshima, Y. Sugita, G. Inesi, C. Toyoshima, Structural role of countertransport revealed in Ca^{2+} pump crystal structure in the absence of Ca^{2+}, Proc. Natl. Acad. Sci. U. S. A. 102 (2005) 14489–14496.
[46] C. Toyoshima, M. Nakasako, H. Nomura, H. Ogawa, Crystal structure of the calcium pump of sarcoplasmic reticulum at 2.6 Å resolution, Nature 405 (2000) 647–655.
[47] C. Toyoshima, H. Nomura, Structural changes in the calcium pump accompanying the dissociation of calcium, Nature 418 (2002) 605–611.
[48] C. Toyoshima, H. Nomura, Y. Sugita, Crystal structures of Ca^{2+}-ATPase in various physiological states, Ann. N. Y. Acad. Sci. 986 (2003) 1–8.
[49] C. Toyoshima, T. Mizutani, Crystal structures of the calcium pump with a bound ATP analogue, Nature 430 (2004) 529–535.

[50] C. Toyoshima, H. Nomura, T. Tsuda, Lumenal gating mechanism revealed in calcium pump crystals structures with phosphate analogues, Nature 432 (2004) 361–368.
[51] C. Olesen, T. Sørensen, R.C. Nielsen, J.V. Moller, P. Nissen, Dephosphorylation of the calcium pump coupled to counterion occlusion, Science 306 (2004) 2251–2255.
[52] T. Sørensen, J.V. Moller, P. Nissen, Phosphoryl transfer and calcium ion occlusion in the calcium pump, Science 304 (2004) 1672–1675.
[53] P. Läuger, R. Benz, G. Stark, E. Bamberg, P.C. Jordan, A. Fahr, W. Brock, Relaxation studies of ion transport systems in lipid bilayer membranes, Q. Rev. Biophys. 14 (1981) 513–598.
[54] H.M. Scofano, A. Vieyra, L. de Meis, Substrate regulation of the sarcoplasmic reticulum ATPase, J. Biol. Chem. 254 (1979) 10227–10231.
[55] L. de Meis, Uncoupled ATPase activity and heat production by the sarcoplasmic reticulum Ca^{2+}-ATPase, J. Biol. Chem. 276 (2001) 25078–25087.
[56] K.A. Dalton, J.D. Pilot, S. Mall, J.M. East, A.G. Lee, Anionic phospholipids decrease the rate of slippage on the Ca^{2+}-ATPase of sarcoplasmic reticulum, Biochem. J 342 (1999) 431–438.
[57] N.W. Seidler, I. Jona, M. Vegh, A. Martonosi, Cyclopiazonic acid is a specific inhibitor of the Ca^{2+}-ATPase of sarcoplasmic reticulum, J. Biol. Chem. 264 (1989) 17816–17823.